



OPEN

Correlation of spinal cord compression angle and increased signal intensity on MRI in patients with ossification of posterior longitudinal ligament

Qi Zhao^{1,3}, Dong Xie^{1,2,3}, Hao Wu^{1,2,3}, Longqing Wang¹, Qing Chen¹, Mingliang Shi¹, Baocheng Niu¹ & Lili Yang¹✉

We retrospectively investigated the correlation between the spinal cord compression angle and increased signal intensity (ISI) in 118 patients with ossification of the posterior longitudinal ligament (OPLL). Patients were analyzed based on the presence and shape of ISI on magnetic resonance imaging. Various indicators, including the spinal cord compression angle, were measured through imaging examinations. Spearman's correlation and logistic regression were used for analyses. Significant positive correlations were observed between the ISI grade and the spinal cord compression angle, maximum spinal canal occupying rate, cervical range of motion, and segmental range of motion. The spinal cord compression ratio and Japanese Orthopaedic Association (JOA) score were negatively correlated with the ISI grade. Regression analysis revealed that the spinal cord compression angle and JOA scores were independent factors that significantly influenced ISI grade. The odds ratio of ISI was 3.858 (95% confidence interval: 0.974–15.278) when comparing the highest and lowest quartiles of the spinal cord compression angle. Patients with a spinal cord compression angle $> 35^\circ$ had more severe imaging manifestations. Thus, a spinal cord compression angle $> 35^\circ$ could serve as a significant indicator of OPLL severity, and greater attention should be focused on treating patients with larger spinal cord compression angles.

Keywords OPLL, Spinal cord compression angle, Increased signal intensity, Imaging factor

Ossification of the posterior longitudinal ligament (OPLL) is a pathological condition characterized by anomalous ossification. Individuals affected by OPLL frequently exhibit clinical manifestations, including neck and shoulder pain, restricted fine motor movements, sensory and motor impairments in the limbs, and, in severe cases, quadriplegia and incontinence. Timely surgical intervention is imperative to prevent irreversible neurological impairment. However, surgical treatment may prove ineffective in cases where muscle atrophy or bladder and bowel dysfunction have already manifested¹.

An increased signal intensity (ISI) on T2-weighted magnetic resonance images (MRIs) indicates local ischemia, edema, inflammation, degeneration, and necrosis of the spinal cord and is clinically important in patients with OPLL². Takahashi et al.³ observed that prolonged spinal cord compression from a herniated intervertebral disc or OPLL leads to significant ISI in the MRI T2-weighted phase. Ischemic spinal injuries are common in severe compressions. Such compression causes spinal cord myelomalacia, evidenced by the “snake-eye” sign in transverse sections, which may worsen and extend the ISI longitudinally⁴. According to previous research, the presence of ISI, particularly long-segment hyperintensity, frequently signifies severe spinal cord injury and is associated with an unfavorable prognosis^{5,6}. Vedantam and Rajshekhar⁷ showed that patients with long-segment ISI had comparatively diminished postoperative efficacy despite undergoing surgical intervention.

¹Spine Center, Department of Orthopaedics, Shanghai Changzheng Hospital, Second Affiliated Hospital of Naval Medical University, Shanghai 200003, China. ²Department of Orthopaedics, PLA Navy No. 905 Hospital, Shanghai 200052, China. ³These authors contributed equally: Qi Zhao, Dong Xie and Hao Wu. ✉email: yangll@smmu.edu.cn

Furthermore, attenuation of the ISI following surgery was correlated with enhanced recovery of neurological function.

ISI within the spinal cord serves as a crucial indicator of neurological function, and its association with clinical effectiveness has been extensively discussed^{8,9}. However, the determinants of ISI remain unclear. Investigating the risk factors associated with the ISI can assist healthcare professionals in more accurately assessing the condition of patients with OPLL, enabling timely consideration of surgical interventions for those with high-risk factors.

The spinal cord compression angle represents a distinct regional kyphotic angle. Notably, previous studies have indicated that cervical kyphosis is a significant prognostic risk factor^{10,11}. Nakashima et al.¹² argue that in terms of clinical prognosis, local kyphosis is more significant than global kyphosis. Additionally, Lee et al.¹³ showed that an increased spinal cord compression angle correlated with heightened symptom severity and a decrease in the Japanese Orthopaedic Association (JOA) score.

Limited research has been conducted on the association between the spinal cord compression angle and incidence of ISI in patients with OPLL. This study aimed to examine the correlation between the spinal cord compression angle and the ISI, which can provide valuable insights for clinicians in assessing patient conditions and determining the urgency of surgical intervention to prevent the onset of ISI.

Results

Demographic data

The demographic characteristics of patients with varying ISI grades were analyzed and compared, as shown in Table 1. The results indicated no statistically significant differences in sex, age, body mass index (BMI), diabetes, hypertension, smoking, or drinking history among the three groups ($P > 0.05$). However, the JOA scores were significantly lower in the grade 1 and 2 ISI groups than in the grade 0 ISI group ($P < 0.001$).

Imaging findings

Upon examining the imaging factors of patients among the three ISI groups (Table 2), no statistically significant disparities were observed in terms of OPLL classification and cervical curvature ($P > 0.05$). The spinal cord compression angle was significantly greater in patients in the grade 1 and 2 ISI groups than in those in the grade 0 ISI group ($P < 0.001$). Additionally, the spinal cord compression ratio was significantly lower in patients in the grade 1 and 2 ISI groups than in those in the grade 0 ISI group ($P < 0.001$). The results indicated that patients in the grade 1 and 2 ISI groups had a significantly higher maximum spinal canal occupying rate than those in the grade 0 ISI group ($P = 0.003$). Additionally, patients in the grade 2 ISI group exhibited greater cervical and segmental ranges of motion than those in the grade 1 and 0 ISI groups ($P = 0.026$ and 0.005 , respectively).

Correlation analysis

No significant correlation was found between sex, age, BMI, OPLL classification, and cervical curvature and the ISI grade ($P > 0.05$). However, the JOA score ($r = -0.370$, $P < 0.001$) and spinal cord compression ratio ($r = -0.379$, $P < 0.001$) were significantly negatively correlated with the ISI grade. Additionally, the spinal cord compression angle ($r = 0.393$, $P < 0.001$), maximum spinal canal occupying rate ($r = 0.317$, $P < 0.001$), cervical range of motion ($r = 0.189$, $P = 0.041$), and segmental range of motion ($r = 0.242$, $P = 0.008$) were positively correlated with the ISI grade (Fig. 1a–f).

Multivariable logistic regression model

The spinal cord compression angle, spinal cord compression ratio, maximum spinal canal occupying rate, cervical range of motion, segmental range of motion, and JOA score were incorporated into the logistic regression analysis. The results revealed that the spinal cord compression angle ($\beta = -0.043$, odds ratio [OR] = 1.044, 95% confidence interval [CI]: 1.004–1.085) and JOA score ($\beta = -0.284$, OR = 0.752, 95% CI: 0.602–0.940) were identified as independent factors influencing ISI grade ($P < 0.05$) (Fig. 2).

	Grade 0 ISI (n = 54)	Grade 1 ISI (n = 42)	Grade 2 ISI (n = 22)	P value
Sex				0.186
Female	31 (57.4)	31 (73.8)	16 (72.7)	
Male	23 (42.6)	11 (26.2)	6 (27.3)	
Age (years)	58.26 ± 10.13	57.69 ± 7.31	57.27 ± 9.44	0.900
BMI	24.56 ± 3.04	25.31 ± 2.70	25.82 ± 3.20	0.198
Diabetes	13 (24.1)	7 (16.7)	4 (18.2)	0.645
Hypertension	22 (40.7)	16 (38.1)	10 (45.5)	0.850
Smoking	14 (25.9)	8 (19.0)	6 (27.3)	0.669
Drinking	4 (7.4)	4 (9.5)	1 (4.5)	0.817
JOA score	11.02 ± 1.97	9.98 ± 1.52 ^a	9.18 ± 1.71 ^a	<0.001

Table 1. Demographic data of the patients. Values are presented as n (%) or mean ± standard error of the mean. ^aComparison with the grade 0 ISI group ($P < 0.05$). ISI, increased signal intensity; BMI, body mass index; JOA, Japanese Orthopaedic Association.

	Grade 0 ISI (n = 54)	Grade 1 ISI (n = 42)	Grade 2 ISI (n = 22)	P value
Spinal cord compression angle (°)	26.34 ± 8.95	34.05 ± 11.52 ^a	36.55 ± 9.49 ^a	< 0.001
Spinal cord compression ratio (%)	30.40 ± 7.12	24.58 ± 6.11 ^a	24.27 ± 6.18 ^a	< 0.001
OPLL type				0.999
Localized	11 (20.4)	9 (21.4)	5 (22.7)	
Segmental	7 (13.0)	6 (14.3)	2 (9.1)	
Continuous	7 (13.0)	6 (14.3)	3 (13.6)	
Mixed	29 (53.7)	21 (50.0)	12 (54.5)	
Cervical curvature				0.208
Lordosis	23 (42.6)	12 (28.6)	11 (50.0)	
Straight	16 (29.6)	13 (31.0)	8 (36.4)	
Kyphosis	15 (27.8)	17 (40.5)	3 (13.6)	
Maximum spinal canal occupying rate (%)	51.86 ± 10.24	58.23 ± 9.79 ^a	59.04 ± 10.66 ^a	0.003
Cervical range of motion (°)	34.05 ± 10.31	34.89 ± 11.41	41.83 ± 14.22 ^{a,b}	0.026
Segmental range of motion (°)	6.69 ± 3.67	7.00 ± 4.01	9.83 ± 3.70 ^{a,b}	0.005

Table 2. Comparative analysis of imaging factors among patients exhibiting varying degrees of ISI. Values are presented as n (%) or mean ± standard error of the mean. ISI, increased signal intensity; OPLL, ossification of the posterior longitudinal ligament. ^aComparisons with the grade 0 ISI group, $P < 0.05$. ^bComparisons with the grade 1 ISI group, $P < 0.05$.

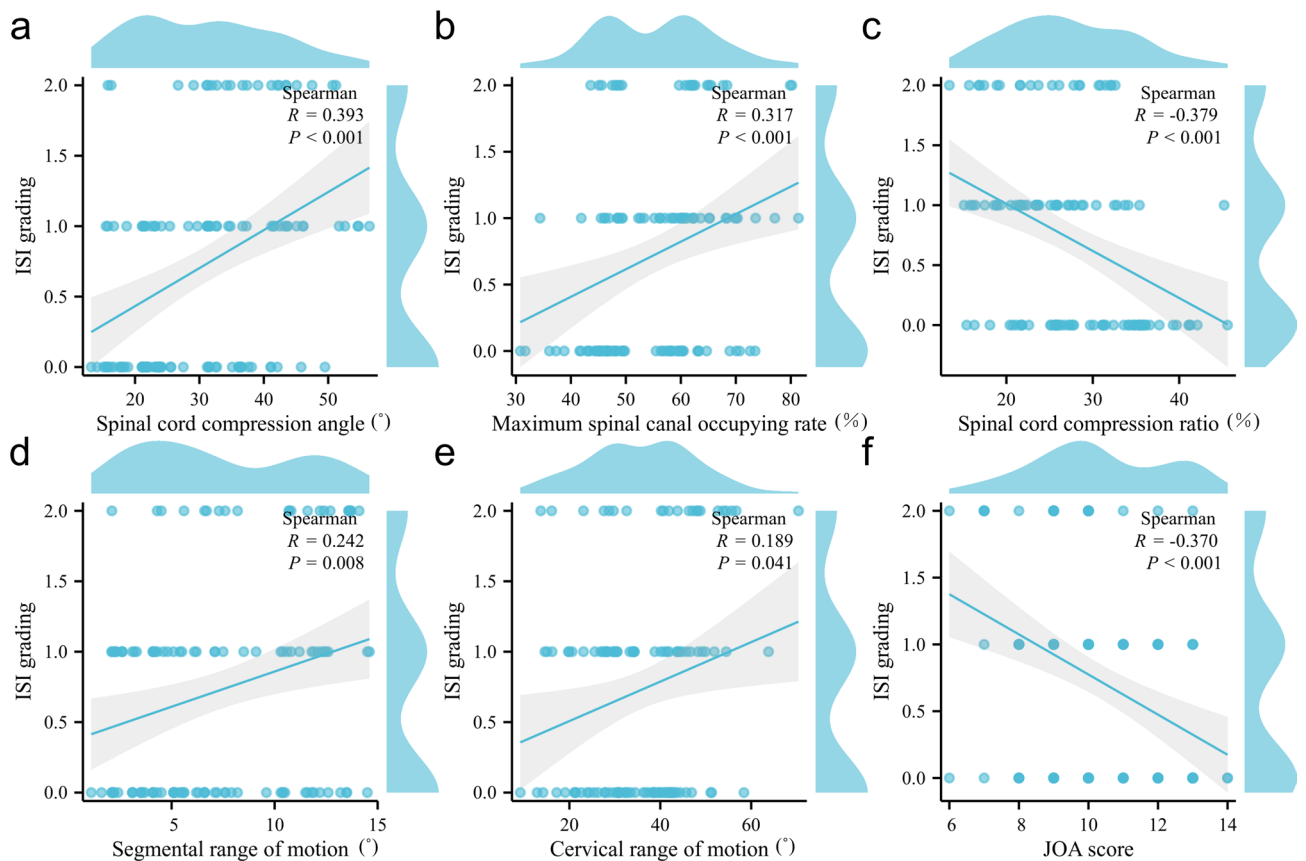


Figure 1. Correlation between the spinal cord compression angle (a), maximum spinal canal occupying rate (b), spinal cord compression ratio (c), segmental range of motion (d), cervical range of motion (e), and JOA score (f) and the ISI grade. ISI, increased signal intensity; JOA, Japanese Orthopaedic Association.

Relationship between the spinal cord compression angle and the ISI

The associations between the spinal cord compression angle and the ISI are presented in Table 3. The crude ORs and 95% CIs of the ISI indicated that the spinal cord compression angle exhibited a significant positive association with the ISI. After adjusting for potential confounding factors, the multivariate-adjusted OR of ISI was 3.858 (95% CI: 0.974–15.278) for the highest quartile versus the lowest quartile of the spinal cord compression angle.

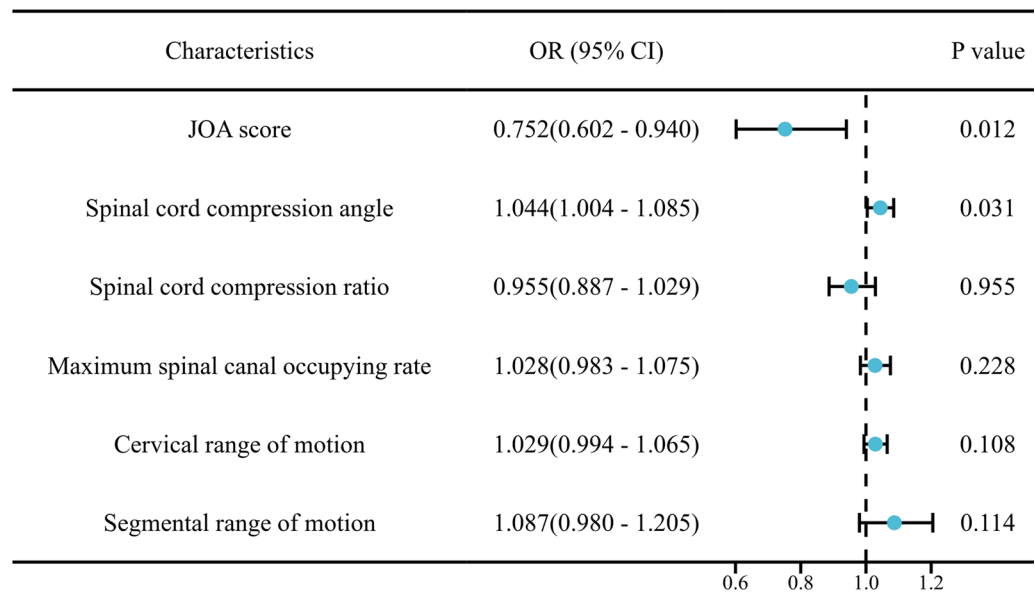


Figure 2. Multivariate logistic regression analysis of factors affecting the increased signal intensity. OR, odds ratio; CI, confidence interval; JOA, Japanese Orthopaedic Association.

Spinal cord compression angle	Participants (n)	Patients with ISI (n)	Crude odds ratio (95% confidence interval)	Multivariate adjusted
Q1 ($\leq 21.7^\circ$)	30	10	1 (reference)	1 (reference)
Q2 (21.8° – 31.3°)	30	14	1.750 (0.616–4.973)	1.383 (0.431–4.436)
Q3 (31.4° – 39.6°)	29	16	2.462 (0.858–7.065)	1.973 (0.603–6.450)
Q4 ($> 39.6^\circ$)	29	24	9.600 (2.816–32.733)	3.858 (0.974–15.278)
P for trend			<0.01	0.046

Table 3. Odds ratios (95% confidence intervals) of ISI by quartiles of spinal cord compression angle. The spinal cord compression angle was categorized into quartiles, with a higher quartile indicating a higher spinal cord compression angle. ISI, increased signal intensity.

Comparison between large- and small-spinal cord compression angle groups

Patients were categorized into large- and small-angle groups based on whether the spinal cord compression angle exceeded 35° and compared (Table 4). The findings revealed that patients in the large-angle group exhibited a lower spinal cord compression ratio ($P < 0.001$), a higher maximum spinal canal occupying rate ($P = 0.006$), a higher prevalence of high-grade ISI ($P = 0.009$), and lower JOA scores ($P = 0.039$) than those in the small-angle group.

Discussion

Multiple factors, including genetic, environmental, and metabolic factors, influence OPLL. This ossification gradually progresses in multiple directions, leading to spinal cord compression. Consequently, individuals may experience symptoms such as numbness, weakness, fine motor impairment, walking instability, and potential limb paralysis. These debilitating effects significantly affect the overall quality of life of patients¹.

Currently, the prevailing consensus among scholars attributes the manifestation of ISI to prolonged mechanical compression and dynamic stimulation injury¹⁴. Mechanical compression of the spinal cord can result from various factors, including intervertebral disc herniation, osteophyte formation, OPLL, and ossification of the ligamentum flavum. These elements exert pressure on the spinal cord, culminating in nerve cell necrosis and myelomalacia. Failure to promptly alleviate compression leads to atrophy of the gray matter in the spinal cord, accompanied by the formation of cavities, ultimately resulting in ISI^{15,16}.

Dynamic stimulation injuries primarily occur during flexion and extension of the cervical spine. The extensive range of motion and inherent instability of the cervical spine result in repetitive friction and stimulation of the spinal cord owing to ossification or osteophytes. Consequently, the spinal cord is repeatedly stimulated, increasing susceptibility to ISI¹⁷. In our study, we identified the spinal cord compression angle, spinal cord compression ratio, maximum spinal canal occupying rate, cervical range of motion, and segmental range of motion as representative indicators.

The presence of ISI in the spinal cord frequently indicates severe nerve damage. Scholars posit that the occurrence of long-segment high signal intensity is often associated with significant spinal cord injury and a poor

	Small-angle group (n = 76)	Large-angle group (n = 42)	P value
Spinal cord compression ratio (%)	29.30 ± 7.14	23.36 ± 5.57	< 0.001
Maximum spinal canal occupying rate (%)	53.33 ± 10.05	59.35 ± 10.62	0.006
Cervical range of motion (°)	35.26 ± 11.00	36.78 ± 11.14	0.506
Segmental range of motion (°)	7.47 ± 4.13	7.25 ± 3.63	0.896
Cervical curvature			0.834
Lordosis	30 (39.5)	16 (38.1)	
Straight	25 (32.9)	12 (28.6)	
Kyphosis	21 (27.6)	14 (33.3)	
ISI			0.009
Grade 0	41 (53.9)	13 (30.9)	
Grade 1	25 (32.9)	17 (40.5)	
Grade 2	10 (13.2)	12 (28.6)	
JOA score	10.59 ± 1.78	9.79 ± 2.02	0.039

Table 4. Comparison between large- and small-spinal cord compression angle groups. Values are presented as n (%) or mean ± standard error of the mean. Large-angle group, spinal cord compression angle ≤ 35°; small-angle group, spinal cord compression angle > 35°. ISI, increased signal intensity; JOA, Japanese Orthopaedic Association.

prognosis^{5,6}. Research has demonstrated that patients exhibiting long segments and prominently highlighted ISI tend to experience unfavorable postoperative outcomes, even after surgical intervention. Conversely, a decrease in ISI after surgery is correlated with improved recovery of neurological function⁷. The initial stages of ISI involve spinal cord edema, subsequent degeneration and necrosis of gray matter cells, and, ultimately, the development of syringomyelia. Timely surgical intervention can alleviate spinal cord compression, leading to notable improvements in spinal cord edema and ischemia. Consequently, certain nerve cell functions may be restored, and the heightened signal intensity in the spinal cord may be diminished or even eradicated¹⁸. Therefore, it is imperative to investigate the factors that influence the ISI.

The study revealed significant negative correlations between the JOA score and spinal cord compression ratio and the ISI grade. Conversely, significant positive correlations were observed between the ISI grade and the spinal cord compression angle, maximum spinal canal occupying rate, cervical range of motion, and segmental range of motion. Logistic regression analysis further identified the spinal cord compression angle and JOA score as independent influencing factors for ISI grade. Additionally, patients in the large-angle group—those spinal cord compression angle greater than 35°—had a lower spinal cord compression ratio, higher maximum spinal canal occupying rate, higher prevalence of high-grade ISI, and lower JOA scores than those in the small-angle group.

Handa et al.¹⁹ observed a notable disparity in the rate of neurological function recovery between patients with preoperative JOA scores < 12 and those with scores ≥ 12. Additionally, Chen et al.²⁰ identified the preoperative JOA score as a significant determinant of postoperative efficacy. Notably, a lower preoperative JOA score corresponds to a more severe spinal cord injury, and once the injury reaches a certain threshold, irreversible pathological changes often occur.

The spinal cord compression ratio and maximum spinal canal occupying rate are reliable indicators of spinal cord compression status. Previous research²¹ has demonstrated that in cases of multisegment compression of the cervical spinal cord, the segment with the highest compression tends to exhibit spinal cord hyperintensity. Furthermore, spinal cord hyperintensities are associated with the degree of compression.

Kadanka et al.²² discovered that the presence of the ISI did not consistently align with the extent of spinal cord compression. In fact, apart from the mechanical compression caused by ossified materials, repetitive dynamic stimulation also contributes to this phenomenon, with cervical spine instability and extensive mobility playing significant roles.

Based on the cross-sectional view of the T2-weighted MRI at the spinal cord's maximal compression level, researchers classified it into three shapes: boomerang, teardrop, and triangular. These observations reveal that patients with a triangular spinal cord shape have the poorest clinical prognosis and an increased incidence of ISI²³. In addition, Lee et al.¹³ showed that a greater angle of spinal cord compression leads to more severe symptoms and adverse effects on the spinal cord, ultimately resulting in a reduction in the preoperative JOA score. Importantly, the spinal cord compression angle has multiple implications. Primarily, it serves as an indicator of the ossification morphology. A larger spinal cord compression angle corresponds to a more acute ossification, thereby subjecting the spinal cord to heightened strain, particularly during neck flexion. Consequently, this heightened strain increases the likelihood of nerve cell necrosis and the manifestation of severe neurological symptoms within a short timeframe. Simultaneously, mirroring the ossification morphology, the spinal cord compression angle can indicate the extent of spinal cord compression. A distinct gap exists between the spinal cord and the cerebrospinal fluid and between the dura mater and the spinal canal. As ossification initiates growth, the spinal cord retains its cushioning space despite its potentially acute configuration, thereby limiting the magnitude of the spinal cord compression angle. As the ossification process persists, stenosis of the spinal canal intensifies, leading to potential compression of the spinal cord. Consequently, the angle of spinal cord compression tends to increase progressively, thereby indicating the extent of spinal cord compression.

Our study demonstrated a significant spinal cord compression angle, especially that greater than 35° , observed on a patient's imaging suggests a higher risk of ISI or a broader ISI range. Therefore, assessing the necessity for surgical intervention becomes crucial. Measuring the spinal cord compression angle aids surgeons in effectively evaluating the severity of OPLL in patients, making it an essential parameter for reflecting OPLL's condition.

This study had certain limitations, including a relatively small sample size and potential selection bias. Consequently, the sample size should be augmented to enhance the statistical robustness of research findings. Additionally, because this study was conducted at a single center, further investigations involving multiple centers are warranted to validate its generalizability. We should also recognize that the assessment of spinal cord compression angle may not always offer a thorough evaluation, especially in instances of atypical ossification shapes, thereby indicating a constraint of this measurement. Nonetheless, in most scenarios, it continues to serve as a beneficial tool for assessment.

In conclusion, greater attention should be focused on treating patients with larger spinal cord compression angles. A spinal cord compression angle exceeding 35° could serve as a significant indicator for assessing the severity of OPLL patients.

Methods

Study population

A retrospective analysis was conducted in a cohort of 118 patients diagnosed with OPLL who underwent surgical intervention at our institution between 2020 and 2021. The cohort comprised 78 men and 40 women, with an average age of 57.9 ± 9.0 years. Ethical approval was obtained from the institutional review board of Shanghai Changzheng Hospital. This study was conducted in accordance with the principles of the Declaration of Helsinki. All the participants provided written informed consent to participate in the study.

Inclusion and exclusion criteria

The diagnostic criteria for cervical OPLL were based on imaging findings and medical history. A comprehensive set of imaging examinations of the cervical spine, including radiography (X-ray), computed tomography (CT), and MRI, was conducted. Patients with spinal cord nerve dysfunction resulting from other diseases, severe medical conditions, malignant tumors, tuberculosis, or concurrent peripheral nerve damage were excluded.

Imaging factors

In the midsagittal position of the T2-weighted MRI, the segment exhibiting the most pronounced compression should be identified, and two tangent lines should be drawn at the vertex of the spinal cord compression. One tangent line should follow the upper incisal edge of the ossification, whereas the other should follow the lower incisal edge. The acute angle formed at the intersection of these two lines represents the angle of spinal cord compression, as shown in Fig. 3. In patients with multilevel ossification, the spinal cord compression angle was measured at the most severely compressed segment. In cases where two or more segments exhibited a similar degree of compression, we measured and averaged the spinal cord compression angles of multiple segments.

Based on the identification and configuration of the ISI observed on T2-weighted MRI, the grading system assigned grade 0 to cases lacking spinal hyperintensity, grade 1 to those exhibiting punctate hyperintensity, and grade 2 to those displaying diffuse hyperintensity (Fig. 4a–c).

Imaging examinations were conducted to measure various parameters, including the maximum spinal canal occupying rate, spinal cord compression ratio, cervical curvature, cervical range of motion, segmental range of motion, and OPLL classification (Fig. 5a–h). The maximum spinal canal occupying rate was defined as the ratio of the maximal ossification thickness to the anteroposterior spinal canal diameter on CT axial imaging. The spinal

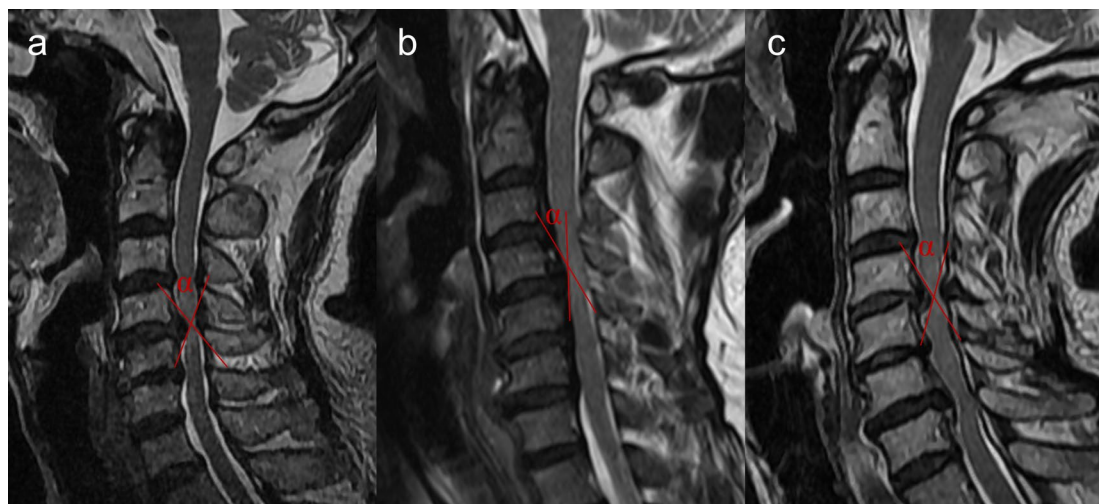


Figure 3. Schematic diagram of the measurement of the spinal cord compression angle in cases of triangular (a), flat (b), and round (c) shapes of ossification of the posterior longitudinal ligament.



Figure 4. Schematic representation of the grading of increased signal intensity: (a) no spinal hyperintensity, grade 0; (b) punctate hyperintensity, grade 1; (c) diffuse hyperintensity, grade 2.

cord compression ratio was measured as the ratio of the anteroposterior diameter to the transverse diameter of the spinal cord on MR axial imaging at the most compressed segment. Cervical curvature was calculated by the Cobb angle between the lines perpendicular to the upper end plate of the C2 vertebral body and the lower end plate of the C7 vertebral body and classified as lordosis ($C2-7$ Cobb angle $> 4^\circ$), straight ($-4^\circ < C2-7$ Cobb angle $\leq 4^\circ$), and kyphosis ($C2-7$ Cobb angle $\leq -4^\circ$). The cervical range of motion refers to the difference between the $C2-7$ Cobb angle on the cervical flexion lateral radiograph and the $C2-7$ Cobb angle on the cervical extension lateral radiograph. The segmental range of motion refers to the difference between the target segment Cobb on the lateral cervical flexion radiograph and the target segment Cobb on the cervical extension lateral radiograph. OPLL was categorized into localized, segmental, continuous, and mixed types based on morphological characteristics. Three orthopedic physicians performed all measurements, and the average of the measurements was used.

Statistical analyses

Data analysis was performed using SPSS version 27 (IBM Corp., Armonk, NY, USA). R language version 4.2.1 (The R Project, Vienna, Austria) was used for graphing. Quantitative data are presented as mean \pm standard error of the mean, and a comparison among the three groups was conducted using analysis of variance. Nonparametric statistical tests were used when the data deviated from a normal distribution. Qualitative data are expressed as n (%), and comparisons among groups were performed using the chi-squared test. Spearman's correlation analysis was used for correlation testing. Logistic regression was used for the univariate and multivariate analyses. Statistical significance was set at $P < 0.05$.

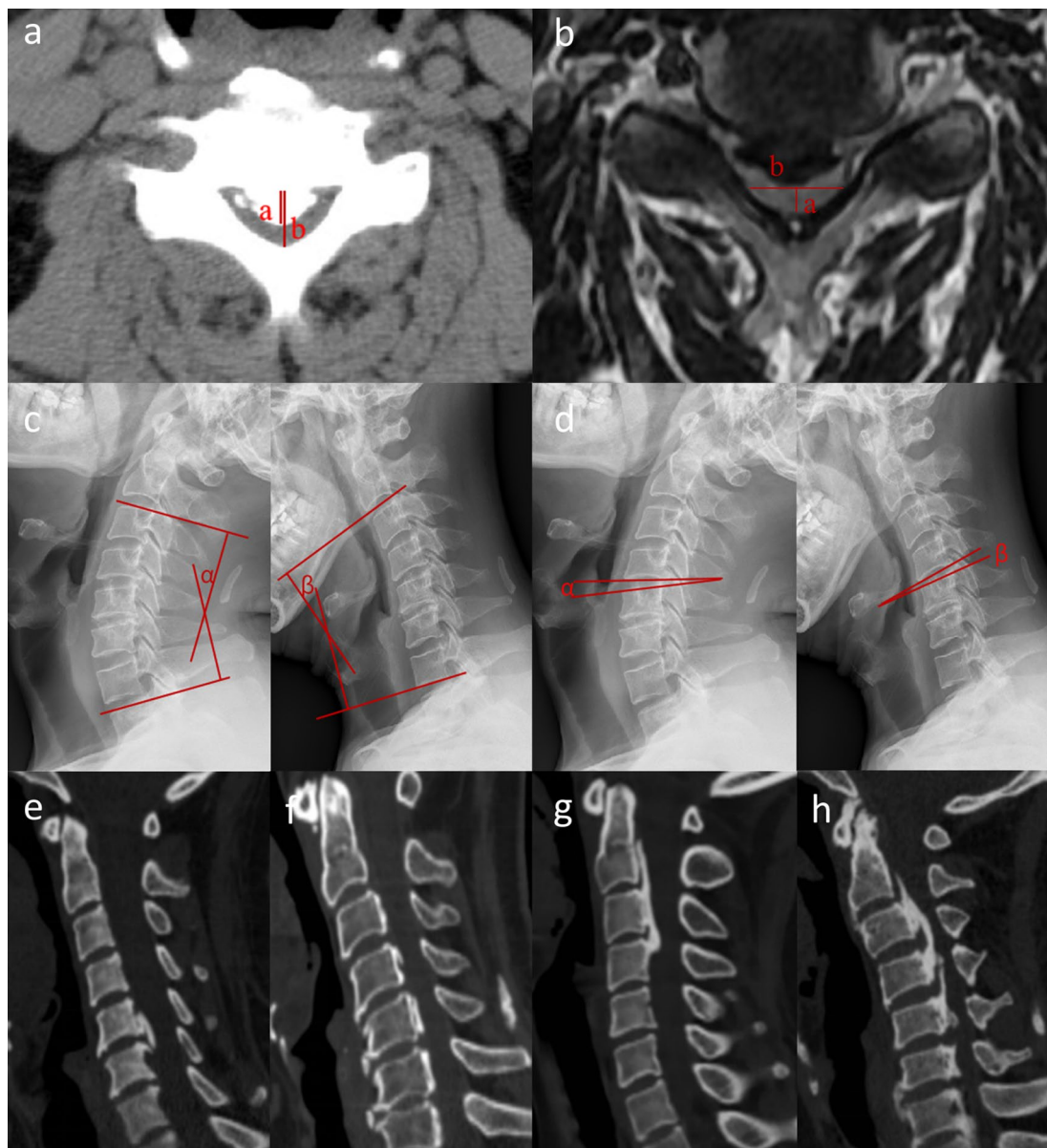


Figure 5. Schematic representation of the maximum spinal canal occupying rate (a), spinal cord compression ratio (b), cervical range of motion (c), segmental range of motion (d), and localized (e), segmental (f), continuous (g), and mixed (h) types of ossification of the posterior longitudinal ligament. Maximum spinal canal occupying rate = $(a/b) \times 100\%$; spinal cord compression ratio = $(a/b) \times 100\%$; cervical range of motion = $\alpha + \beta$; segmental range of motion = $\alpha + \beta$.

Data availability

The datasets generated during and/or analyzed during the current study are available from the corresponding author on reasonable request.

Received: 6 January 2024; Accepted: 31 July 2024

Published online: 03 August 2024

References

1. Boody, B. S., Lendner, M. & Vaccaro, A. R. Ossification of the posterior longitudinal ligament in the cervical spine: A review. *Int. Orthop.* **43**, 797–805 (2019).
2. Alafifi, T., Kern, R. & Fehlings, M. Clinical and MRI predictors of outcome after surgical intervention for cervical spondylotic myelopathy. *J. Neuroimaging* **17**, 315–322 (2007).
3. Takahashi, M. *et al.* Increased MR signal intensity secondary to chronic cervical cord compression. *Neuroradiology* **29**, 550–556 (1987).
4. Al-Mefty, O. *et al.* Myelopathic cervical spondylotic lesions demonstrated by magnetic resonance imaging. *J. Neurosurg.* **68**, 217–222 (1988).

5. Choi, J. H. *et al.* Does intramedullary signal intensity on MRI affect the surgical outcomes of patients with ossification of posterior longitudinal ligament?. *J. Korean Neurosurg. Soc.* **56**, 121–129 (2014).
6. Fernández de Rota, J. J. *et al.* Cervical spondylotic myelopathy due to chronic compression: The role of signal intensity changes in magnetic resonance images. *J. Neurosurg. Spine* **6**, 17–22 (2007).
7. Vedantam, A. & Rajshekhar, V. Does the type of T2-weighted hyperintensity influence surgical outcome in patients with cervical spondylotic myelopathy? A review. *Eur. Spine J.* **22**, 96–106 (2013).
8. Miyazaki, M. *et al.* Relationship of preoperative intramedullary MRI signal intensity and dynamic factors with surgical outcomes of laminoplasty for cervical ossification of the posterior longitudinal ligament. *Clin. Neurol. Neurosurg.* **174**, 117–122 (2018).
9. Qizhi, S. *et al.* Factors associated with intramedullary MRI abnormalities in patients with ossification of the posterior longitudinal ligament. *J. Spinal Disord. Tech.* **28**, E304–E309 (2015).
10. Chiba, K. *et al.* Long-term results of expansive open-door laminoplasty for cervical myelopathy—average 14-year follow-up study. *Spine (Phila Pa 1976)* **31**, 2998–3005 (2006).
11. Suda, K. *et al.* Local kyphosis reduces surgical outcomes of expansive open-door laminoplasty for cervical spondylotic myelopathy. *Spine (Phila Pa 1976)* **28**, 1258–1262 (2003).
12. Nakashima, H. *et al.* Prediction of outcome following surgical treatment of cervical myelopathy based on features of ossification of the posterior longitudinal ligament: A systematic review. *JBJS Rev.* **5**, e5 (2017).
13. Lee, N. *et al.* Compression angle of ossification of the posterior longitudinal ligament and its clinical significance in cervical myelopathy. *J. Korean Neurosurg. Soc.* **59**, 471–477 (2016).
14. Iyer, A., Azad, T. D. & Tharin, S. Cervical spondylotic myelopathy. *Clin. Spine Surg.* **29**, 408–414 (2016).
15. Yagi, M. *et al.* Long-term surgical outcome and risk factors in patients with cervical myelopathy and a change in signal intensity of intramedullary spinal cord on magnetic resonance imaging. *J. Neurosurg. Spine* **12**, 59–65 (2010).
16. Baptiste, D. C. & Fehlings, M. G. Pathophysiology of cervical myelopathy. *Spine J.* **6**, 190S–197S (2006).
17. Rao, R. Neck pain, cervical radiculopathy, and cervical myelopathy: Pathophysiology, natural history, and clinical evaluation. *J. Bone Joint Surg. Am.* **84**, 1872–1881 (2002).
18. Ito, T. *et al.* Cervical spondylotic myelopathy. Clinicopathologic study on the progression pattern and thin myelinated fibers of the lesions of seven patients examined during complete autopsy. *Spine (Phila Pa 1976)* **21**, 827–833 (1996).
19. Handa, Y. *et al.* Evaluation of prognostic factors and clinical outcome in elderly patients in whom expansive laminoplasty is performed for cervical myelopathy due to multisegmental spondylotic canal stenosis. A retrospective comparison with younger patients. *J. Neurosurg.* **96**, S173–S179 (2002).
20. Chen, Y. *et al.* Surgical results and prognostic factors of anterior cervical corpectomy and fusion for ossification of the posterior longitudinal ligament. *PLOS ONE* **9**, e102008 (2014).
21. Kameyama, T. *et al.* Intramedullary high intensity lesion on T2-weighted MR images in compressive cervical myelopathy. *Rinsho Shinkeigaku* **31**, 1177–1181 (1991).
22. Kadanka, Z. *et al.* Cross-sectional transverse area and hyperintensities on magnetic resonance imaging in relation to the clinical picture in cervical spondylotic myelopathy. *Spine (Phila Pa 1976)* **32**, 2573–2577 (2007).
23. Matsuyama, Y. *et al.* Cervical myelopathy due to OPLL: Clinical evaluation by MRI and intraoperative spinal sonography. *J. Spinal Disord. Tech.* **17**, 401–404 (2004).

Acknowledgements

The authors thank all the study participants.

Author contributions

Q.Z. analyzed the data and wrote the manuscript. D.X. and H.W. collected and analyzed the data. L.W., Q.C., M.S., and B.N. collected the data and participated in the design of the study. L.Y. was responsible for funding acquisition, designed the research, and revised the manuscript.

Funding

This study was sponsored by the National Natural Science Foundation of China (82372431), Shanghai Municipal Health Commission Health Leading Talents Program (2022LJ007), Natural Science Foundation of the Science and Technology Commission of Shanghai Municipality (22ZR1476700), Shanghai Municipal Annual Innovative Medical Device Application Demonstration Project (23SHS05700-06), Fifth Round Innovation Team of Shanghai Changning District, and Open Bidding for Selecting the Best Candidates cultivation project of Shanghai Changzheng Hospital (2023YJBF-PY10).

Competing interests

The authors declare no competing interests.

Additional information

Correspondence and requests for materials should be addressed to L.Y.

Reprints and permissions information is available at www.nature.com/reprints.

Publisher's note Springer Nature remains neutral with regard to jurisdictional claims in published maps and institutional affiliations.

Open Access This article is licensed under a Creative Commons Attribution-NonCommercial-NoDerivatives 4.0 International License, which permits any non-commercial use, sharing, distribution and reproduction in any medium or format, as long as you give appropriate credit to the original author(s) and the source, provide a link to the Creative Commons licence, and indicate if you modified the licensed material. You do not have permission under this licence to share adapted material derived from this article or parts of it. The images or other third party material in this article are included in the article's Creative Commons licence, unless indicated otherwise in a credit line to the material. If material is not included in the article's Creative Commons licence and your intended use is not permitted by statutory regulation or exceeds the permitted use, you will need to obtain permission directly from the copyright holder. To view a copy of this licence, visit <http://creativecommons.org/licenses/by-nc-nd/4.0/>.

© The Author(s) 2024